

## ORIGINAL ARTICLE

Wnt/ $\beta$ -catenin activation and macrophage induction during liver cancer development following steatosis

A Debebe<sup>1</sup>, V Medina<sup>1,12</sup>, C-Y Chen<sup>1</sup>, IM Mahajan<sup>1,12</sup>, C Jia<sup>1,2,12</sup>, D Fu<sup>3,12</sup>, L He<sup>1</sup>, N Zeng<sup>1,12</sup>, BW Stiles<sup>4</sup>, C-L Chen<sup>5</sup>, M Wang<sup>6</sup>, K-R Aggarwal<sup>1</sup>, Z Peng<sup>1</sup>, J Huang<sup>1</sup>, J Chen<sup>1</sup>, M Li<sup>1</sup>, T Dong<sup>1</sup>, S Atkins<sup>1</sup>, Z Borok<sup>7,8,9</sup>, W Yuan<sup>5</sup>, K Machida<sup>5</sup>, C Ju<sup>6</sup>, M Kahn<sup>1,8,9</sup>, D Johnson<sup>10</sup> and BL Stiles<sup>1,9,11</sup>

Obesity confers an independent risk for carcinogenesis. In the liver, steatosis often proceeds cancer formation; however, the mechanisms by which steatosis promotes carcinogenesis is unknown. We hypothesize that steatosis alters the microenvironment to promote proliferation of tumor initiating cells (TICs) and carcinogenesis. We used several liver cancer models to address the mechanisms underlying the role of obesity in cancer and verified these findings in patient populations. Using bioinformatics analysis and verified by biochemical assays, we identified that hepatosteatosis resulting from either *Pten* deletion or transgenic expression of HCV core/NS5A proteins, promotes the activation of Wnt/ $\beta$ -catenin. We verified that high fat diet lipid accumulation is also capable of inducing Wnt/ $\beta$ -catenin. Caloric restriction inhibits hepatosteatosis, reduces Wnt/ $\beta$ -catenin activation and blocks the expansion of TICs leading to complete inhibition of tumorigenesis without affecting the phosphatase and tensin homologue deleted on chromosome 10 (PTEN) loss regulated protein kinase B (AKT) activation. Pharmacological inhibition or loss of the Wnt/ $\beta$ -catenin signal represses TIC growth *in vitro*, and decreases the accumulation of TICs *in vivo*. In human liver cancers, ontology analysis of gene set enrichment analysis (GSEA)-defined Wnt signature genes indicates that Wnt signaling is significantly induced in tumor samples compared with healthy livers. Indeed, Wnt signature genes predict 90% of tumors in a cohort of 558 patient samples. Selective depletion of macrophages leads to reduction of Wnt and suppresses tumor development, suggesting infiltrating macrophages as a key source for steatosis-induced Wnt expression. These data established Wnt/ $\beta$ -catenin as a novel signal produced by infiltrating macrophages induced by steatosis that promotes growth of tumor progenitor cells, underlying the increased risk of liver tumor development in obese individuals.

*Oncogene* (2017) 36, 6020–6029; doi:10.1038/onc.2017.207; published online 3 July 2017

## INTRODUCTION

Obesity is a major factor for the development of a variety of human cancers yet the mechanisms underlying this association are poorly understood.<sup>1</sup> This correlation is particularly strong in liver cancer where males with a body mass index > 35 have a 4.52 fold higher incidence of liver cancer.<sup>2</sup> Approximately 80% of liver cancer patients have underlying liver disease that display lipid metabolic dysfunction.<sup>3</sup> In this study, we used liver cancer as a model system to address the contribution of obesity to cancer.

In two major liver diseases (alcoholic and non-alcoholic fatty liver diseases) that manifest steatosis, inflammatory hepatitis develops at later stages of disease progression.<sup>4</sup> Hepatitis C infection, an inflammatory condition, is accompanied with steatosis development.<sup>5</sup> These conditions underlie liver cancer development and suggest that accumulation of lipids in hepatocytes may alter the microenvironment to produce signaling molecules that support tumor growth. However, the molecular mechanisms by which steatosis leads to tumorigenesis is still poorly understood. In this study, we used several animal models to determine how steatosis alters the tumor microenvironment to

regulate tumor initiating cell (TIC) growth and tumorigenesis. In mice lacking *Pten* (phosphatase and tensin homologue deleted on chromosome 10), the negative regulator of the insulin/phosphatidylinositol 3-kinase (PI3K) signaling pathway, steatosis is required for tumor development.<sup>6–10</sup> In hepatitis C core or NS5A protein transgenic models, high fat diet (HFD) feeding accelerates tumorigenesis.<sup>11</sup> Using these models and genetic and dietary approaches to block steatosis, we defined Wnt produced from macrophages as a key tumor microenvironment factor that is induced by intracellular lipid accumulation and the resultant steatosis. The induction of Wnt results from macrophage accumulation and promotes the expansion of the transformed liver TICs to mediate the progression of tumorigenesis.

## RESULTS

Blocking steatosis abolishes tumor development in *Pten*-null livers To first investigate the role of lipid accumulation in tumor development, we employed a liver cancer model (*Pten*<sup>loxP/loxP</sup>; *Alb-Cre*<sup>+</sup>, *Pten* null) system where steatosis proceeds spontaneous

<sup>1</sup>Pharmacology and Pharmaceutical Sciences, School of Pharmacy, University of Southern California, Los Angeles, CA, USA; <sup>2</sup>Department of Nuclear medicine, Shanghai 10th people's hospital, Tongji University, Shanghai, China; <sup>3</sup>Central Laboratory for Medical Research, Shanghai 10th People's Hospital, Tongji University School of Medicine, Shanghai, China; <sup>4</sup>Jet Propulsion Laboratory, California Institute of Technology, Pasadena, CA, USA; <sup>5</sup>Molecular Microbiology and Immunology, Keck School of Medicine, University of Southern California, Los Angeles, CA, USA; <sup>6</sup>Pharmaceutical Sciences, Skaggs School of Pharmacy and Pharmaceutical Sciences, University of Colorado, Aurora, CO, USA; <sup>7</sup>Will Rogers Institute Pulmonary Research Center, Medicine, Keck School of Medicine, University of Southern California, Los Angeles, CA, USA; <sup>8</sup>Biochemistry and Molecular Biology, Keck School of Medicine, University of Southern California, Los Angeles, CA, USA; <sup>9</sup>Norris Comprehensive Cancer Center, University of Southern California, Los Angeles, CA, USA; <sup>10</sup>Department of Molecular and Cellular Biology, Baylor College of Medicine, Houston, TX, USA and <sup>11</sup>Pathology, Keck School of Medicine, University of Southern California, Los Angeles, CA, USA. Correspondence: Dr BL Stiles, Pharmacology and Pharmaceutical Sciences, USC School of Pharmacy, PSC 402, 1985 Zonal Ave. Los Angeles, CA 90089, USA. E-mail: bstiles@usc.edu

<sup>12</sup>These authors contributed equally to this work.

Received 14 December 2016; revised 28 April 2017; accepted 21 May 2017; published online 3 July 2017

tumor formation.<sup>6,7,9,10,12,13</sup> In this model, peri-central vein steatosis develops as early as before 1 month of age and all hepatocytes are laden with lipids by 3 months of age. The mice starts to develop hyperplasia phenotype after 6 months and tumors are observed starting at 7–8 months of age. All mice develop spontaneous tumors by 12 months of age. In these mice, caloric restriction (CR) abolished liver lipid accumulation and completely blocked tumorigenesis (Figure 1, Supplementary Figure S1 and Table 1). In addition, AKT2, the major isoform of protein kinase B (AKT) in the liver has been shown to regulate lipid metabolism rather than cell survival.<sup>14–16</sup> Deletion of *Akt2* attenuated liver steatosis developed in the *Pten*-null mice<sup>6,7</sup> and resulted in >80% reduction in tumor incidence (Figure 1 and Table 1). Mice lacking both Phosphatase and tensin homologue deleted on chromosome 10 (PTEN) and AKT2 eventually developed steatosis after 6–9 months of age, likely due to peripheral insulin resistance reported for mice with AKT2 loss.<sup>14</sup> This steatosis development may have contributed to the eventual development of tumors in some of these mice. Previous work has shown that the effect of AKT2 is independent of the potential survival kinase activity that it may possess.<sup>6</sup> Together, these data strongly implicate that steatosis is necessary for tumor progression.

Steatosis induces Wnt signaling

To address how steatosis in *Pten*-null mice may promote tumor formation, we next compared unbiased differential gene expression analyses in livers of *Pten*-null mice (steatotic-cancer model) with those in the two non-steatotic models, that is, *Pten/Akt2* double mutant Dm mice (GSE70501) and the CR-fed *Pten*-null mice (GSE data pending submission) (Figure 1b and Supplementary Figure S2). Our analysis led to the discovery of Wnt signature genes that are upregulated by PTEN loss and

downregulated by either *Akt2* deletion or CR (Figure 1b and Supplementary Figure S2).

To confirm the array data, we first validated the expression of several Wnt ligands and receptors in the *Pten*-null livers vs controls (Figure 2a). Consistent with Wnt activation, expression of  $\beta$ -catenin, the intracellular effector of Wnt signaling was observed at tumor regions and the periductal area where pre-malignant TIC activation is observed (Figures 2b and c and Supplementary Figure S3). Increased phosphorylation of LRP6 at Ser-1490 demonstrated a ligand-dependent activation of Wnt signaling has occurred in the *Pten*-null livers. The p-S552 form of  $\beta$ -catenin is also higher in the *Pten*-null liver lysates, indicative of activated  $\beta$ -catenin (Figure 2c). Phosphorylation at S552 induces  $\beta$ -catenin accumulation in the nucleus where it regulates transcription of target genes.<sup>17</sup> Consistently, increased expression of  $\beta$ -catenin targets Axin2, C-Myc, Jag1 and CD44 is observed, suggesting  $\beta$ -catenin transcriptional activity is induced in the *Pten*-null livers (Figure 2d). Transcriptional activity of  $\beta$ -catenin is also induced in the periductal area as evidenced by the presence of  $\beta$ -galactosidase when the *Pten*-null mice were crossed with the BAT-Gal  $\beta$ -catenin transcriptional activity reporter mice (Figure 2e).

**Table 1.** Tumor incidence in CR and *Akt2*-deleted *Pten*-null mice vs controls

	Control	<i>Pten null</i>
Ad lib (13 months)	0/10	7/7
CR (3months+10months CR)	0/10	0/7
<i>Akt2</i> wild type (> 12months)	0/10	26/26
<i>Akt2</i> deleted (> 12 months)	0/10	6/48

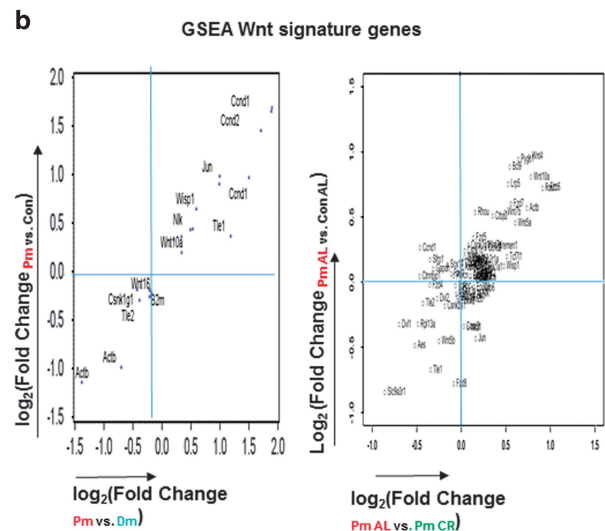
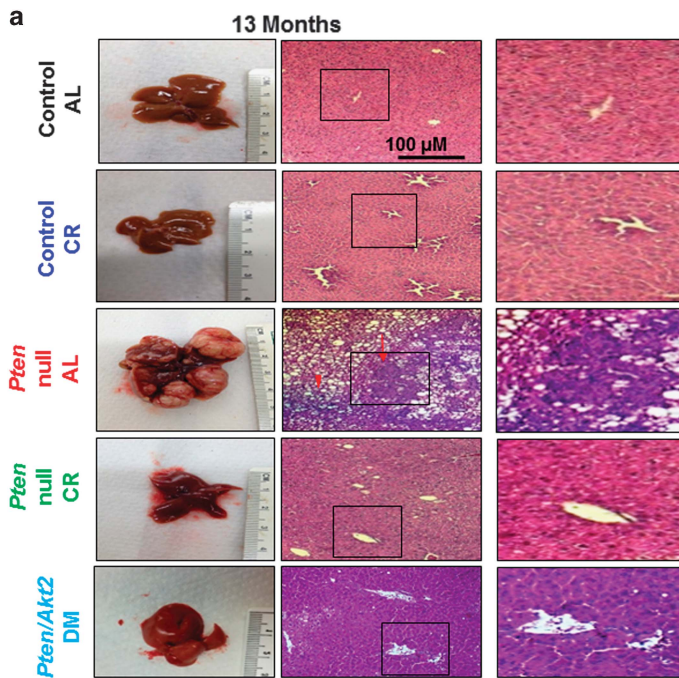


**Figure 1.** Blocking steatosis inhibits tumor development in *Pten*-null livers and alters Wnt signaling. **(a)** Liver tissue sections were collected from 13-month-old control (Con), *Pten*-null (Pm) and *Pten/Akt2* double null (*Pten/Akt2*, Dm) mice. *Pten*-null mice were fed either *ad libitum* (AL) or calorie restriction (CR) diet. Left, macroscopic images of livers. Right, microscopic images of liver tissue sections showing both hepatocytes and cholangiocytes in the tumor. *n* = 6–11. **(b)** Wnt signature genes that are differentially expressed in *Pten*-null (Pm) livers and altered by deletion of *Akt2* (double mutant, Dm) and CR. The majority of the Kyoto Encyclopedia of Genes and Genomes (KEGG) Wnt signature genes found altered by *Pten* deletion were found to be reversed by *Akt2* deletion (left) or CR (right). Data collected from microarray analysis of Pm vs Dm (Top) and RNA-seq analysis of Pm AL, vs Pm CR (Bottom). *n* = 3–5.

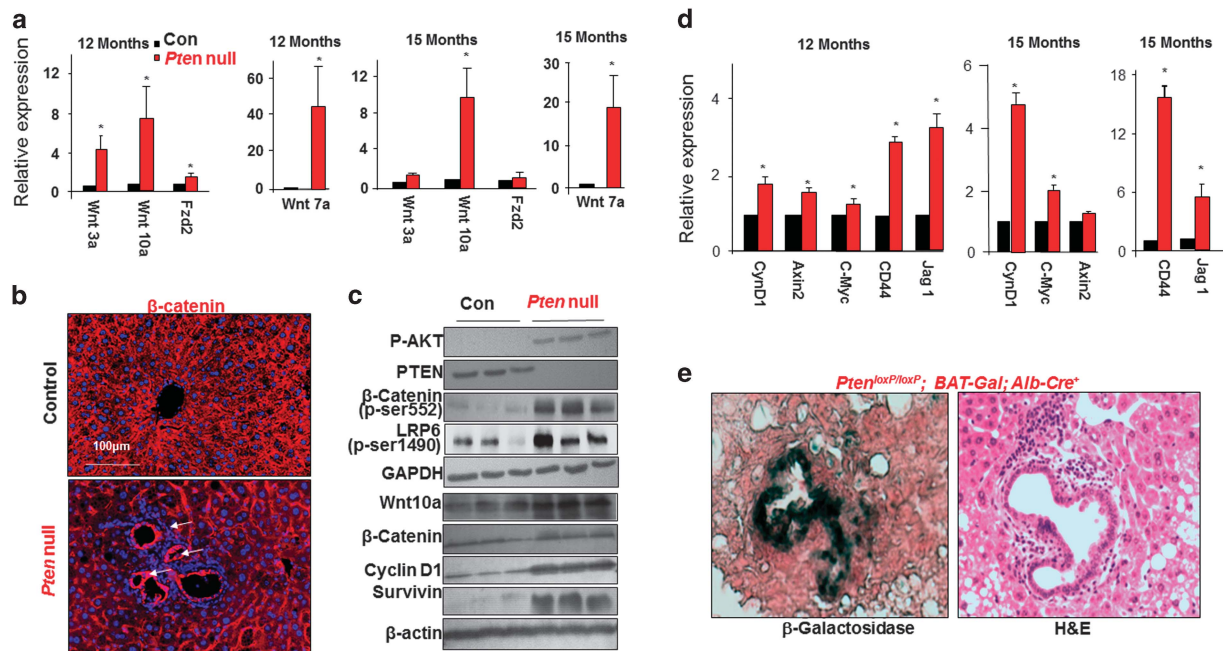


**Figure 2.** Wnt signaling is induced in steatotic *Pten*-null livers. **(a)** Quantitative PCR analysis for the expression of Wnt ligands and receptors in livers of *Pten*-null and control mice.  $n = 5$ . \* Indicates significant difference from controls at  $P \leq 0.05$ . **(b)**  $\beta$ -catenin staining (red) in control and *Pten*-null mice.  $\beta$ -catenin is expressed throughout the normal liver. Its levels are increased in the *Pten*-null livers at the hyperplastic ductal region where the progenitor cell niche is located (arrow). Blue, 4',6-diamidino-2-phenylindole (DAPI). Representative of three animals. **(c)** Immunoblotting analysis of PTEN signal and Wnt signal in livers from 12-month-old mice. Glyceraldehyde 3-phosphate dehydrogenase (GAPDH) and  $\beta$ -actin are loading controls. **(d)** Quantitative PCR analysis of Wnt target genes in control and *Pten*-null livers.  $n = 3-5$ . \* Indicates significant difference from controls at  $P \leq 0.05$ . **(e)**  $\beta$ -galactosidase activity was detected in the periductal area (dark greenish blue staining in left panel) in the 6-month-old *Pten*-null liver carrying BAT-Gal reporter construct. Right panel, hematoxylin & eosin (H&E) staining in adjacent section. Representative of three animals.

These results demonstrate that Wnt activity is indeed induced at the progenitor cell niche following chronic steatosis and this increase continues as the *Pten*-null livers start to develop tumors. This observation supports an idea that Wnt may serve as an early competency factor induced by steatosis to promote the establishment of tumors.

In addition, we examined Wnt signaling in two non-PTEN-related models where steatosis precedes cancer development. Similar to the *Pten*-null liver cancer model, transgenic expression of hepatitis C virus (HCV) core or NS5A protein leads to hepatosteatosis early in life with tumors eventually develop in a portion of the male mice. High fat diet feeding for 12 months increases the tumor burden from 10 to 50%.<sup>11,18</sup> Gene profiling (GSE61435) analysis showed that Wnt signaling is induced in livers of either HCV core or NS5A transgenic mice fed HFD (Figure 3a). Quantitative PCR analysis verified these findings (Figures 3a and b). To further test if steatosis can induce Wnt signals without genetic manipulation of PTEN or HCV, we evaluated Wnt expression in wild-type mice fed HFD, which led to increased lipid accumulation (Supplementary Figure S4). Increases in  $\beta$ -catenin staining intensity, mRNA expression for Wnt 10a and their transcriptional targets survivin and CD44 are both observed with HFD feeding (Figure 3c). In addition, both total  $\beta$ -catenin and activated  $\beta$ -catenin (pSer552) were increased by HFD feeding (Figure 3d). Thus, steatosis alone is likely sufficient to induce Wnt signals, though to a lesser extent (Figure 3c). While induction of phospho-S552  $\beta$ -catenin is indicative of the involvement of AKT,<sup>17</sup> AKT's involvement in this HFD-induced activation of  $\beta$ -catenin is inconclusive due to individual variations (Figure 3d).

We have observed that deletion of *Akt2*<sup>5,7</sup> and CR both attenuate steatosis (Supplementary Figure S1). We show here that AKT2 loss and CR also both repress Wnt signals (Figures 4a and b). This effect of CR does not appear to be mediated by its

role on AKT or AMPK as AKT and AMPK phosphorylation in *Pten*-null livers is not altered by CR treatment (Figure 4c). Phosphorylation of Erk is reduced by CR. How this reduced Erk phosphorylation may play a role in CR-mediated Wnt signal repression is not clear. Regardless, these data reveal that in models where steatosis occurs, that is, *Pten*-null, HCV core or HCV NS5A transgenics, Wnt induction precedes tumorigenesis. When steatosis is inhibited in either the *Pten/Akt2* DM or CR mice, Wnt inhibition correlates with reduction or abolishment of tumor development. These observations implicated a novel role for Wnts as potential mediators for fatty liver-induced liver cancer development.

#### Steatosis leads to TIC accumulation

In liver cancer, the presence of TICs accounts for the high cellular heterogeneity, challenging therapeutic treatment.<sup>19,20</sup> TICs have also been shown to contribute to tumor development in the *Pten*-null mice.<sup>6,13</sup> In order to define these TIC populations in our model systems, we used CD133 and CD49f, cell surface markers often used to identify liver TICs.<sup>13,18</sup> In both *Akt2*-deleted and CR-fed *Pten*-null mice, the number of CD133 and CD49f dual positive or CD133 single positive TICs are reduced compared to that observed in the *Pten*-null mice (Figures 5a and b). Deletion of *Akt2* returned the numbers of TICs to the same levels as controls (Figure 5a). When *Pten*-null mice were subjected to a CR diet, the TIC populations are reduced by 50% (Figure 5b). Concurrent with the reduction of the TIC population, expression of EpCam, K19, AFP and Trop2, stemness markers for liver TICs<sup>19,20</sup> are also significantly reduced by CR treatment (Figure 5c). Accordingly, HFD feeding alone, which results in liver steatosis (Supplementary Figure S4), also increased the expression of some of these markers for TICs (data not shown). Collectively, these data support the idea that blocking fatty liver formation with CR or *Akt2* deletion leads to reduced accumulation of hepatic TICs.

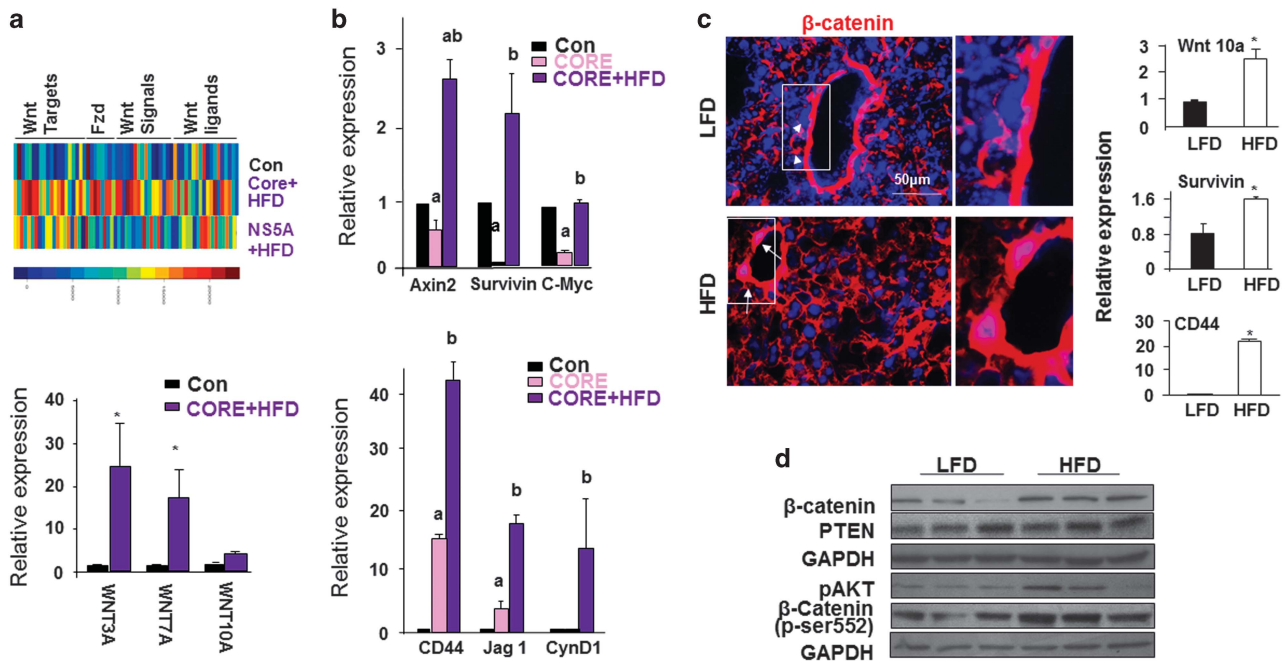


**Figure 3.** Wnt signaling is induced in steatotic livers induced by HCV transgene and high fat feeding. (a) Top, Heat map of Wnt signaling gene changes observed in HFD-fed HCV core and NSSA transgenic livers vs controls. Animals were fed on HFD for 12 months. Scale bar for heat color is shown at the bottom where blue indicates low expression and red indicates high expression. Bottom, Quantitative PCR analysis for the expression of Wnt ligands in the same mice.  $n = 5$ . \* Indicates significant difference from controls at  $P \leq 0.05$ . (b) Quantitative PCR analysis for the expression of Wnt target genes in the HFD-fed HCV core transgenic livers vs controls.  $n = 5$ . a, Indicates significant difference from controls at  $P \leq 0.05$ . b, Indicates significant difference from Core transgenic group at  $P \leq 0.05$ . (c) Left,  $\beta$ -catenin staining in 3-month-old animals fed HFD vs LFD for 9 months. Arrow, nuclear staining of  $\beta$ -catenin in periductal cells in HFD mice; arrow head, membrane staining in periductal cells in LFD mice. Representative of three animals. Right, Quantitative PCR analysis of Wnt ligand and target genes.  $n = 3-6$ . \* $P \leq 0.05$ . (d) Western blot analysis of molecules in the PI3K/AKT and Wnt/ $\beta$ -catenin pathways in liver lysate from LFD- and HFD-fed mice.

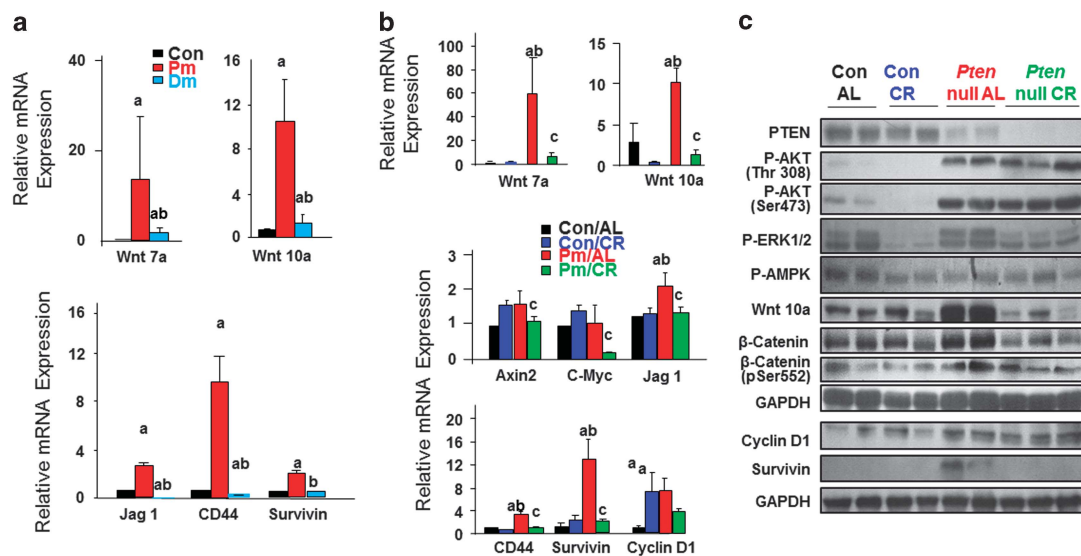


**Figure 4.** Wnt signaling is reduced when steatosis is inhibited. (a) AKT2 loss results in reduced expression of Wnt ligands and target genes,  $n = 3-5$ . a, difference from Con; b, difference from Pm.  $P \leq 0.05$ . 9-month-old mice. (b) mRNA expression levels of Wnt ligands and target genes in CR vs ad Lib-fed control and *Pten*-null liver.  $n = 3-5$ . a, difference from Con/AL; b, difference from Con/CR; c, different from Pm/AL.  $P < 0.05$ . 3-month-old animals were put on CR diet for 10 months. (c) Protein expression analysis of liver samples from the indicated treatment groups.

**Inhibiting Wnt signaling blocks TIC activation**

The Wnt family of soluble factors is known for their function in establishing niche signals that potentiate the self-renewal of tissue progenitor cells and  $\beta$ -catenin has been characterized as the mediator for this function.<sup>21</sup> To address the potential effects of the

increased Wnt in the *Pten* null livers, we explored whether inhibiting the canonical Wnt/ $\beta$ -catenin attenuates the expansion of TICs. We performed loss-of-function analysis using a pharmacological inhibitor of Wnt signaling. ICG-001 is a small molecule inhibitor that blocks the interaction of  $\beta$ -catenin with cAMP

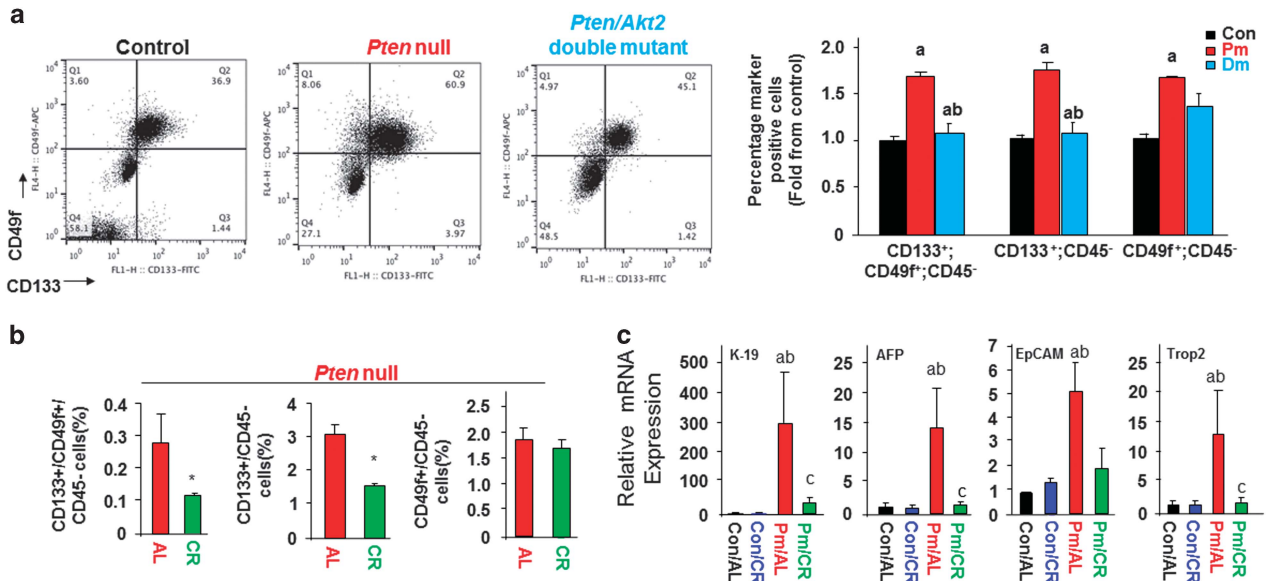


**Figure 5.** Inhibiting steatosis blocks accumulation of TICs. **(a)** Representative flow cytometric (FACS) plot of TICs in *Pten*-null (Pm) vs *Pten/Akt2* double mutant (Dm) mice using CD49f and CD133 to identify TICs. Left, Representative FACS plot; Right, quantitative analysis.  $n = 4-5$ . \* Significantly different from controls at  $P \leq 0.05$ . 9-month-old mice. **(b)** Quantification of FACS analysis of TIC populations in AL ( $n = 6$ ) and CR ( $n = 7$ )-fed *Pten*-null mice. \* Significantly different from AL at  $P \leq 0.05$ . 3-month-old animals were put on CR diet for 10 months. **(c)** Hepatic TIC markers are induced in Pm/AL mice and blocked with CR.  $n = 6-11$ . a, significantly different from control. b, significantly different from Pm.  $P \leq 0.05$ .

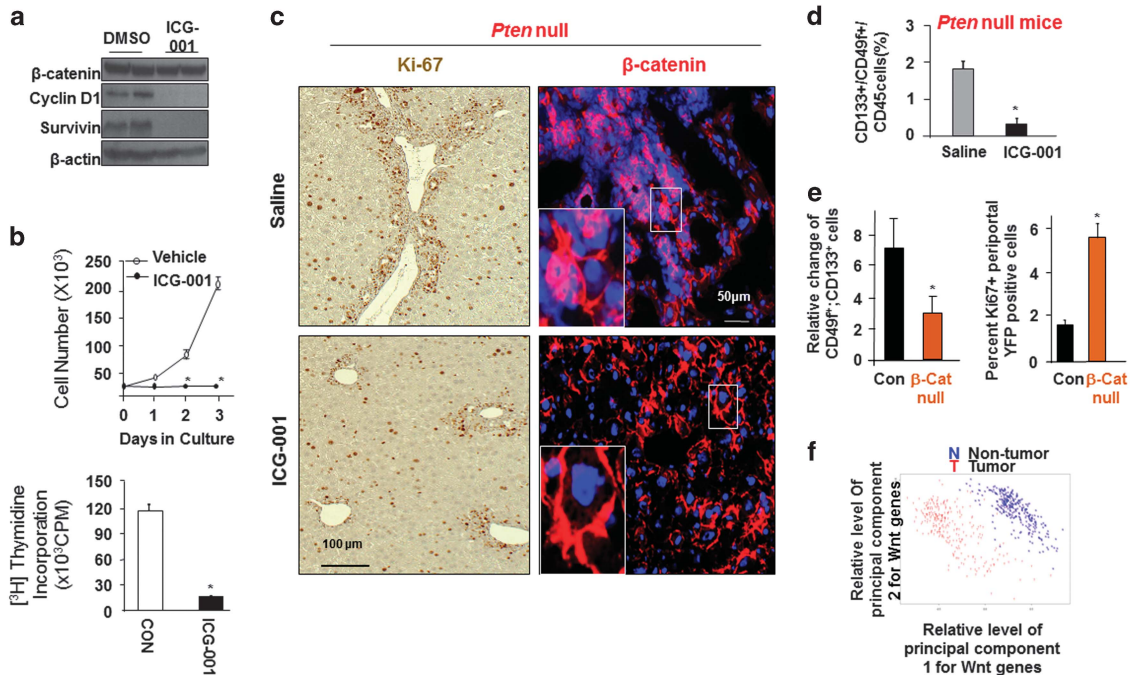


**Figure 6.** Regulation of liver TICs by Wnt/ $\beta$ -catenin and in human liver cancer. **(a)** ICG-001 treatment blocks  $\beta$ -catenin transcriptional activity in TICs isolated from patients.  $n = 3$ . **(b)** Growth curve and thymidine incorporation indicates reduced cell growth and proliferation with ICG-001 treatment.  $n = 3$ . \*significantly different from control at  $P \leq 0.05$ . **(c)** Ki-67 (brown nuclei) and  $\beta$ -catenin (red) staining of periductal regions demonstrate quiescent TIC niche in ICG-001 treated livers. One-month-old mice were implanted with pump containing ICG-001 and fed DDC diet to enrich TIC. Representative of at least three animals. **(d)** Quantitative flow cytometry analysis reveals a reduction of CD133<sup>+</sup> and CD49f<sup>+</sup> progenitor cells upon ICG-001 treatment in *Pten*-null mice. **(e)** Left, quantitative flow cytometry analysis reveals a reduction of CD133<sup>+</sup> and CD49f<sup>+</sup> progenitor cells upon deletion of  $\beta$ -catenin.  $\beta$ -catenin mice were pretreated with DDC to enrich the TIC population. Right, quantitation of Ki67 staining in mice lacking  $\beta$ -catenin.  $n = 4$ . \*Indicates values that are significantly different from saline or control group at  $P \leq 0.05$ . **(f)** Principal component analysis of gene expression in human liver tumor vs non-tumor using gene set enrichment analysis-defined Wnt genes as signature.

binding protein.<sup>22</sup> Treatment with ICG-001 in human and mouse TICs reduced  $\beta$ -catenin activity and led to cytostasis (Figures 6a and b). *Pten*-null mice were then treated with ICG-001 to block  $\beta$ -catenin activity *in vivo* (Supplementary Figure S5). Histological analysis of tissue slides showed reduced cell clusters and mitotic activity at the periductal area where the progenitor cell niche is found in the liver (Figure 6c). In addition,  $\beta$ -catenin staining is also intensified at the cell clusters. Flowcytometry (FACS) analysis showed that ICG-001 treatment led to a significant decrease in the CD133+/CD49f+ dual positive TIC cell population (Figure 6d and Supplementary Figure S6A). Reduced expression of TIC markers (AFP, K19, EpCAM and TROP 2) with ICG-001 treatment confirms that inhibiting of  $\beta$ -catenin led to reduced TIC accumulation (Supplementary Figure S6B).  $\beta$ -catenin plays a key role in maintaining hepatocyte biology and normal liver structure.<sup>23</sup> To avoid the complications of chronic  $\beta$ -catenin inhibition in hepatocytes that may result in liver toxicity, we deleted  $\beta$ -catenin in Sox9-positive cells after mature onset ( $\beta$ -catenin loxP/loxP; Sox9-CreER) (Supplementary Figure S6C). Sox9-positive cells have been suggested to be the putative progenitor cells for the liver.<sup>24,25</sup> In this model, deletion of  $\beta$ -catenin also led to reduced TIC cell population and reduced cell proliferation at the periductal progenitor cell niche (Figure 6e and Supplementary Figure S6D). As reduced number of TICs is associated with reduction of steatosis and inhibition of tumor burden (Figures 1 and 5), these findings indicate that inhibiting the steatosis-induced Wnt/ $\beta$ -catenin signal may have the potential to block tumor development.

#### Wnt signaling is induced in human HCC

To validate the biological significance of these results, we screened a gene expression data set collected from human liver cancer specimens (GSE25097)<sup>26,27</sup> that contains 558 samples including 268 tumor samples. Principal component analysis shows that expression of Wnt signaling genes as a group serves as reliable classifiers that separate tumor vs non-tumor samples (Figure 6f). In 10 pairs of human HCC vs adjacent tissues, we validated the protein levels of Wnt 7a, 10a and cyclin D1 in tumors compared with non-tumor tissues (Supplementary Figure S7A). Wnt molecules are also moderately induced in fatty liver tissues. In a separate cohort of HCC patient samples that were independently analyzed by the Human Protein Atlas (<http://www.proteinatlas.org>), higher expression of Wnt ligands (Wnt 7a and 10a) were also found to be concurrent with lower expression of DDK and sFRP, two negative regulators of Wnt signaling (Supplementary Figure S7B). These data verify that as the phenotypes progress from fatty liver to the appearance of tumors, the Wnt signal is progressively induced, further supporting a role of Wnt as a mediator of steatosis-induced tumorigenesis.

#### Macrophages serves as sources for Wnt production

To determine how fatty liver induces Wnt production, we performed gene expression analysis of the *Pten*-null livers where steatosis drives cancer development.<sup>6</sup> Gene ontology analysis using Ingenuity Pathway Analysis softwares of genes shows that two out of the 10 top most significantly altered pathways by *Pten* loss are related to inflammation, that is, leukocyte extravasation and chemokine signaling (Supplementary Figure S8A). Accumulation of cellular lipid is known to produce/induce intracellular signaling factors with both pro- and anti-inflammatory functions in adipose tissue.<sup>4</sup> The *Pten*-null steatotic liver is heavily infiltrated with inflammatory cells (Supplementary Figure S8B). Expression of a number of cytokines, including interleukin-1 $\beta$ , tumor necrosis factor  $\alpha$ , interleukin-6 and monocyte chemotaxis protein 1 are also induced in the *Pten*-null liver (Supplementary Figure S8C), indicating an inflammatory environment. We isolated the non-parenchymal (NPC) CD45+ inflammatory cells from the *Pten*-null

livers and found that they express high levels of Wnt as early as 5 months of age (Supplementary Figure S8D). To further narrow down the cell type that is responsible for inducing Wnt and promoting tumor formation, we quantified the cell compositions in the NPC CD45+ cell population (Supplementary Figure S8E). Both an increase of macrophages and decrease of CD4<sup>+</sup> Th cells were consistently observed with these cell populations as the *Pten*-null mice progress from steatosis to cancer.

To validate this observation, we determined the macrophage populations in the *Pten*-null steatotic livers vs Controls and *Pten*/*Akt2* double mutant livers where steatosis do not occur. A significant increase of macrophages (F4.80 positive) was consistently found in the *Pten*-null livers vs controls as early as 5 months of age (Figure 7a). In accord with a steatosis-driven increase, this population is diminished when *Akt2* is simultaneously deleted (Figure 7a). Supporting this idea, in other mouse models where steatosis occurs (ethanol and HCV infection), immunohistostaining for CD68, a macrophage marker is also more intense as steatosis proceeds (Supplementary Figure S9A). The CD68+ macrophages also accumulated in both human HCC and cholangiocyte carcinoma samples (Supplementary Figure S9B).

To determine whether the macrophages in the *Pten*-null livers produce Wnts, we analyzed Wnt expression in macrophages isolated from mice with different genotypes. This analysis shows that macrophages isolated from the *Pten*-null livers indeed highly express Wnt ligands (Figure 7a). We further stained for Wnt 7a and CD68. Wnt7a and CD68 are closely co-localized in 10 out of 10 randomly selected sections the *Pten*-null livers whereas only 1 out of 10 sections were found to express CD68 and Wnt in close proximity in the control livers or in the livers without steatosis in the *Pten*/*Akt2* double mutants or CR-fed *Pten*-null mice (Figure 7b). These macrophages are also closely localized to the periductal region where the putative TICs are found (Supplementary Figure S10). Thus, the Wnt ligands are produced, at least in part, by the accumulated macrophages in the *Pten*-null liver. This can potentially block the differentiation of TICs and provide the niche *in vivo* that allows their growth into tumors.

To specifically test whether macrophage activation in the *Pten*-null livers play a role in Wnt production and tumorigenesis, we used a liposome-based delivery of chondronate (CLD) to deplete phagocytic cells, that is, macrophages in 6.5–7 month-old mice (Supplementary Figure S11). Liposome delivery of chondronate for 2 months successfully depleted macrophages as indicated by FACS analysis of F4.80/CD11b-positive cells from the spleen and the liver (Supplementary Figures S10A and B). Reduced CD68 staining further confirms macrophage depletion in the livers of *Pten*-null mice (Supplementary Figure S10C). In the *Pten*-null livers, expression of several Wnt ligands are reduced upon macrophage depletion (Figure 7c). At the end of the experiments when the mice are 8–9 months of age, small tumor nodules start to be visible in majority of the *Pten*-null mice (Figure 7d), similar to what we observed previously.<sup>6</sup> When the macrophages are depleted, concurrent with the reduction of Wnt, no visible tumor nodules are observed (Figure 7d). Only two out of the seven mice treated with CLD developed microscopic tumors whereas three out of four untreated mice developed tumors and most are visible macroscopically (Table 2). Together, these results support the idea that a key production source of Wnts in the liver during steatosis is macrophage.

#### DISCUSSION

Tumor mortality and incidence is higher in obese individuals with lipid metabolic dysfunction. This association is particularly high in liver cancer where 80% of cancer occurs in patients with underlying fatty liver disease.<sup>3</sup> Fatty liver is characterized by aberrant lipid accumulation in the liver resulting from sedentary lifestyle, calorie rich diets or alcohol consumption. Hepatitis virus

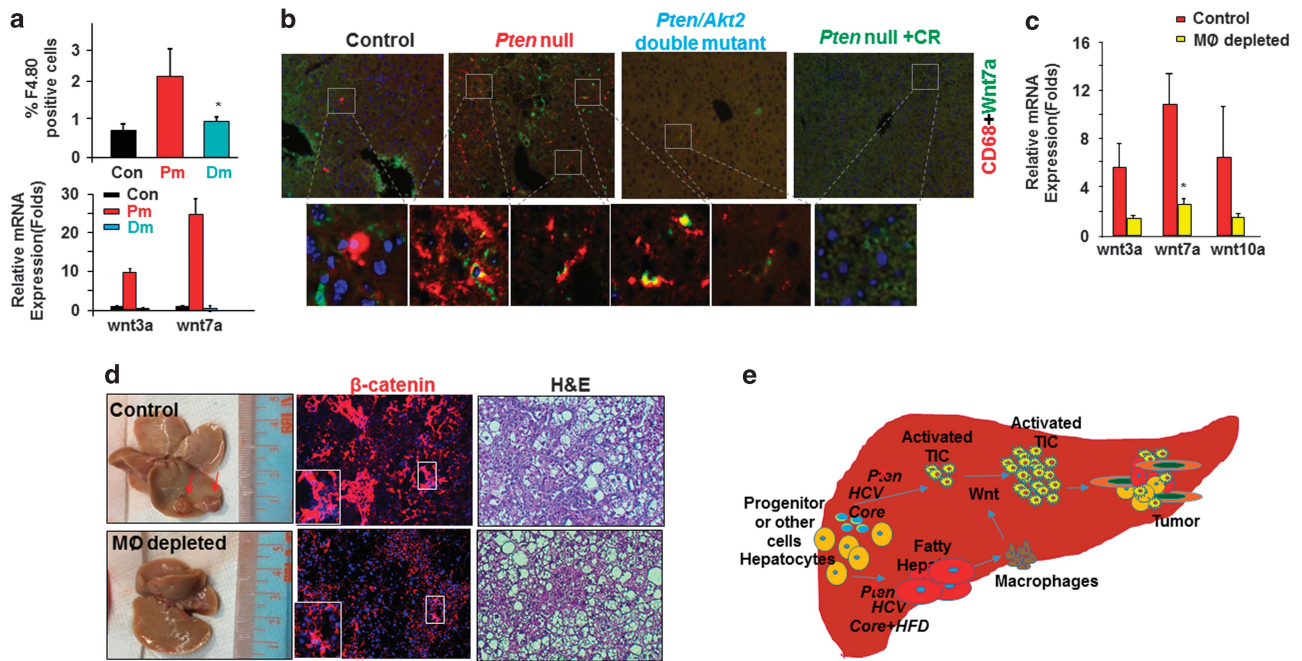


**Figure 7.** Macrophages are potential sources of Wnt induced by steatosis. (a) Top, increase of macrophage population in *Pten*-null mice and its inhibition by deletion of *Akt2* to block steatosis.  $n = 3-4$ . \*significantly different from control at  $P \leq 0.05$ . Bottom, increased expression of two Wnt ligands in *Pten*-null mice and its inhibition by deletion of *Akt2*.  $n = 6$ . \*significantly different from control at  $P \leq 0.05$ . 5-month-old mice. (b) Immunohistostaining shows close localization of Wnt7a (green) and macrophage marker CD68 (red). 9–12-month-old mice. (c) Expression of Wnt ligands and liver phenotypes with macrophage (MØ) depletion.  $n = 3-4$ . \*significantly different from control at  $P \leq 0.05$ . 7-month-old mice were given CLD or vehicle for 2 months. (d) Left, macroscopic images of livers from *Pten*-null mice with or without macrophage depletion. Arrow, tumor nodules developed in the *Pten*-null livers without macrophage depletion. Middle,  $\beta$ -catenin staining in livers from *Pten*-null mice with or without macrophage depletion. Right panel, microscopic images show tumors developed in the *Pten* mice without macrophage depletion (Control) vs lack of tumors with macrophage depletion. (e) Schematic representation of the working model that steatosis promotes tumor progression through Wnt.

**Table 2.** Chronic macrophage depletion by lipo-CLD in *Pten*-null liver cancer

Genotype	Control		<i>Pten null</i>	
	Lipo-PBS	Lipo-Clid	Lipo-PBS	Lipo-Clid
Treatment	Lipo-PBS	Lipo-Clid	Lipo-PBS	Lipo-Clid
Tumor Incidence	0/3	0/4	3/4	2/7

infection, also leads to a steatosis phenotype.<sup>5</sup> However, the molecular mechanisms by which the accumulation of lipids and resultant steatosis leads to tumorigenesis is poorly understood. Our recent work established that the tumor suppressor PTEN-regulated phosphatidylinositol 3-kinase/AKT pathway controls both the positive and negative transcriptional regulators of *de novo* lipogenesis.<sup>7,12,28,29</sup> Using animal models lacking PTEN and the metabolic kinase AKT2,<sup>6</sup> we established that this pro-lipogenic effect is necessary for tumorigenesis to occur in these mice. Here, using a non-genetic CR approach, we further establish that intracellular lipid accumulation is required for tumorigenesis. In these and HCV models, we investigated the molecular mechanisms underlying the steatosis-driven tumor development. While *Akt2* deletion inhibits tumor development, this does not appear to be dependent on its function as a pro-growth/survival kinase.<sup>6</sup> Similarly, CR which completely blocked tumor development did not alter AKT phosphorylation in the *Pten*-null livers. This observation is consistent with the notion that the primary role of CR is decreasing circulating IGF-1, which signals through the phosphatidylinositol 3-kinase /AKT pathway.<sup>30</sup> In this scenario,

decreased circulating IGF-1 due to CR cannot lead to down-regulation of AKT due to PTEN loss as AKT is constitutively active. Another previously demonstrated effect of CR is induction of p-AMPK, which has been proposed to play a role in tumorigenesis by regulating energy metabolism.<sup>31</sup> In our study, CR did not alter p-AMPK amounts, suggesting that it does not play a role inhibiting tumorigenesis. Our collective data are consistent with a key role for Wnt signaling in steatosis-driven tumorigenesis. First, Wnt signal is robustly induced as steatosis develops in mice with *Pten* deletion or in HCV/NS5A transgenics under HFD. Second, Wnt expression is increased by HFD feeding to wild-type mice. Third, Wnt expression is decreased when steatosis is inhibited with CR or *Akt2* deletion. Fourth, downregulation of Wnt occurs with inhibition of tumor development in the CR and *Akt2*-deleted mice. Finally, inhibition of Wnt target  $\beta$ -catenin blocks activation of TICs in the *Pten*-null mice. Collectively, these data support a novel role for Wnt signaling in steatosis-induced tumorigenesis.

In contrast to prior studies that showed oxidative stress accompanies fatty liver phenotype and may act as a genotoxic agent to promote tumorigenesis,<sup>3</sup> our current study establishes a novel role for steatosis in driving tumorigenesis by the recruitment of macrophages that induce Wnt signals. This steatosis-induced Wnt/ $\beta$ -catenin signal is significant to human HCC as upregulation of Wnt expression is strongly associated with human liver cancers, which is in addition to the reported frequent  $\beta$ -catenin activating mutations.<sup>32</sup> PTEN loss and HCV+HFD-induced steatosis are each capable of stimulating the expression of Wnts and activating  $\beta$ -catenin while promoting tumorigenesis. AKT2 loss and CR-mediated inhibition of steatosis led to reduced  $\beta$ -catenin expression and activation concurrent with diminished or

abolished tumor development. Thus, our results reveal that the Wnt/ $\beta$ -catenin signal is induced during steatosis-driven liver cancer development. This upregulation of Wnt expression maybe important for tumor development as Wnt signatures genes can predict tumors vs non-tumors in human samples.

The Wnt family of soluble factors is characterized as niche signals that potentiates the self-renewal of tissue progenitor cells.<sup>21</sup> Studies in embryonic stem cells showed that interactions of  $\beta$ -catenin with coactivators such as cAMP binding protein is associated with undifferentiated stem cell phenotypes.<sup>33</sup> In the intestinal crypt and hair follicle bulge, the presence of Wnt and the activation of  $\beta$ -catenin are necessary for maintaining progenitor cell identity.<sup>34,35</sup> Our study demonstrates that TICs progressively accumulate in the steatotic liver in the *Pten*-null mice with high Wnt expression. On the other hand, downregulation of Wnt is associated with reduced accumulation of TICs and decreased expression of TIC markers in the CR and *Akt2*-deleted livers. High fat diet feeding alone also presented limited ability to induce the expression of some Wnt signals and markers associated with TICs. When the canonical Wnt signal is blocked by targeting  $\beta$ -catenin, tumor cell growth *in vitro* and *in vivo* were both inhibited, revealing that Wnt/ $\beta$ -catenin is a major niche factor that maintains TIC growth and survival.

Given that depletion of macrophages significantly reduces Wnt expression and tumorigenesis, we identify macrophages as one important source of Wnt. Consistent with our mouse models, human fatty liver disease, commonly associated with obesity, encompasses histological features including hepatic steatosis, steatohepatitis, fibrosis and cirrhosis and is often accompanied by infiltration of inflammatory cells including macrophages.<sup>36</sup> Our results are of important clinical significance as tumor intrinsic activation of  $\beta$ -catenin leads to resistance to monoclonal antibody therapy against the programmed death ligand-1 (PD-L1) or programmed cell death protein-1 (PD-1) immune check point therapy.<sup>37–39</sup> One potential mechanism for the promising therapeutic effects of PD-1 therapy so far seen in multiple cancer types<sup>37,40–42</sup> is their ability to inhibit the activation of macrophages.<sup>42</sup> The fact that tumors with activated  $\beta$ -catenin are resistant to such therapy<sup>38,39</sup> suggests that the efficacy of these therapies may be through their ability to inhibit the Wnt/ $\beta$ -catenin signal, consistent with a potential role for macrophage-mediated production of Wnts.

How steatosis specifically induces the activation and/or recruitment of macrophages remains to be determined. In the *Pten*-null livers, there is increased LDL secretion coupled with high oxidative stress conditions.<sup>6,43</sup> Consistent with this observation, we also detected increased LDL receptor expression in macrophages isolated from the *Pten*-null livers (data not shown). The presence of high levels of oxidized LDL (ox-LDL) may serve as a chemotaxis signal that recruits or stimulates the macrophages. An example where lipid particles activate macrophages has been previously reported during atherosclerosis development where phagocytosis of ox-LDL particles by activated macrophages leads to plaque formation.<sup>44</sup> In addition to a direct LDL signal, IL-1 $\beta$  may induce Wnt signaling and support tumor cell growth in colon cancer cells.<sup>45</sup> As IL-1 $\beta$  is strongly induced in the *Pten*-null livers (Supplementary Figure S8), enhanced IL-1 $\beta$  signaling may also contribute to Wnt expression induction. Future studies are needed to fully elucidate the mechanisms by which steatosis induces Wnt secretion from macrophages.

The majority of human liver cancers develop as a result of a progression of diseases that initiates with fatty liver disease resulting from a robust accumulation of intracellular hepatic lipids. Our results provide a new mechanistic understanding by which intracellular lipid accumulation in the liver promotes tumorigenesis. The increase in lipid accumulation leads to steatosis and the infiltration of macrophages resulting in enhanced expression of Wnts and the activation of Wnt/ $\beta$ -catenin signaling (Figure 7e).

This then leads to the accumulation of TICs and tumorigenesis. These findings importantly establish a new link that explains the strong epidemiological association between obesity and cancer.

## MATERIALS AND METHODS

### Patient samples

Patient samples used for this study were coded archival available from tissue bank. All samples were from patients treated with surgery only. The study was conducted with approvals from Shanghai 10th People's Hospital, Tongji University School of Medicine.

### Animals

The mice used in this study have been previously characterized: *Pten*<sup>loxP/loxP</sup>; *Alb-Cre*<sup>+</sup> (*Pten* null, Pm),<sup>9</sup> *Pten* and *Akt2* double mutants (*Dm*)<sup>6,7</sup> and hepatitis C core and NS5A transgenic mice.<sup>11</sup> For reporting  $\beta$ -catenin transcriptional activity, the *Pten*<sup>loxP/loxP</sup>; *Alb-Cre*<sup>+</sup> mice were crossed with BAT-Gal mice carrying seven repeats of the  $\beta$ -gal promoter luciferase reporter construct. Targeted deletion of  $\beta$ -catenin was achieved by crossing *Ctnnb*<sup>loxP/loxP</sup> mice (Jackson, Bar Harbor, ME, USA) with *Sox9-CreER*<sup>+</sup> mice.<sup>46</sup> Deletion of  $\beta$ -catenin is induced by subcutaneous injection of Tamoxifen (5 mg/40 g BW, Sigma Aldrich, St Louis, MO, USA) for three doses every other day at 1 month of age ( $\beta$ -cat null). All animals were housed in a temperature, humidity and light-controlled room (12-h light/dark cycle), allowing free access to food and water. All experimental procedures were approved by the Institutional Animal Care and Use Committee (IACUC) guidelines at the University of Southern California.

### Diets

For the HFD experiment, 3-month-old mice were given 60 kcal% fat diet (06414-Harlan laboratories, Indianapolis, IN, USA) with 10.5 kcal% of fat as low fat diet control (98247 Harlan laboratories) for 9 months. For the CR experiment, control and *Pten*-null mice received either free access to food (*ad libitum*, AL) or CR diet. Calorie restriction was defined as reducing daily caloric intake (calories/day) by 40% relative to average AL intake with a diet that includes similar relative proportions of micronutrients (TestDiet). The CR mice were gradually restricted to 60% of AL intake over 3 weeks. Diet started at 3 months of age and continued for a 10-month duration.

### Drug treatment *in vivo*

Mini osmotic pumps (Alzet model # 1004) containing ICG-001 (30 mg/pump) or saline were implanted subcutaneously on the back of the *Pten*-null mice at 1 month of age. The estimated ICG-001 delivery daily is about 0.8 mg/day.

### Cell culture

A mouse hepatic TIC cell line was established by isolating the CD133<sup>+</sup> non-parenchymal cells.<sup>13</sup> Human TICs were obtained from surgically removing HCC tumors by isolating the CD133<sup>+</sup> non-parenchymal cells.<sup>47</sup> Cell growth was monitored with cell count and [<sup>3</sup>H] thymidine incorporation.

### Microarray, RNA-seq and bioinformatics

mRNAs extracted from liver tissues from 9 months old control, *Pten* null, or *Dm* mice were submitted to Penn State Hershey University Microarray Functional Genomics Core facility for mouse mRNA Microarray analysis using Illumina single color array platform. mRNA extracted from liver tissues from control, control-CR *Pten*-null and *Pten*-null-CR mice were used for RNA-seq analysis in the USC genomics core facility. Unpaired Student's *t*-test was used to analyze differentially expressed genes (> 2 folds) among the different groups. Log transformed microarray data, RNA-seq data and CTGA data from the various models are analyzed for Wnt and inflammatory gene signatures (Supplementary Table s3). For CTGA data, principal component analysis is applied using Wnt genes to determine whether tumors and non-tumors can be classified by these genes.

### Biochemical, molecular biology assays, immunopathology and flow cytometry analysis

Folch method was used to extract hepatic lipid by adding chloroform/methanol (2/1). The supernatant was used for triglyceride (TG) assay using



TG (GPO) Reagent Set (Thermo, Waltham, MA, USA) and the pellets were used for DNA extraction as reported.<sup>6</sup> Plasma ALT was determined using ALT Reagent (Raichem, San Diego, CA, USA) as previously described.<sup>6</sup> qPCR, immunoblotting, immunoprecipitation and immunohistochemistry analysis are performed as described.<sup>6</sup> CD133<sup>+</sup>CD45<sup>-</sup> TICs and CD45<sup>+</sup> immune cells were analyzed using flow cytometry. Primer and antibody information is provided in Supplementary Tables S1 and S2.

### Statistical analysis

Sample sizes are predetermined statistically. Differences between two sample groups are determined using Student's *t*-tests. Multigroup comparisons were performed using Multivariate ANOVA analysis followed by Newman-Keuls pairwise comparison assuming equal variances ( $P \leq 0.05$  was considered to be significant. Data are presented as mean  $\pm$  s.e.m.

### CONFLICT OF INTEREST

The authors declare no conflict of interest.

### ACKNOWLEDGEMENTS

We acknowledge the technical support from Ms Mungoma, Carrithers, Zhang, Barsky and Mr Li, Dr Bryan W Stiles would like to state that 'this work was done as a private venture and not in the author's capacity as an employee of the Jet Propulsion Laboratory, California Institute of Technology'. This work was supported by NIH grants R01CA154986-01 (BLS). Dr Stiles also acknowledges support from NIDDK (R01DK084241-01). Dr Borok was supported by NIH grant R01 HL112638-01. Dr Machida would like to acknowledge NIH grants 1R01AA018857 and P50AA11999. We acknowledge support from USC center for Liver Disease (P30DK48522) and Norris Comprehensive Cancer Center (P30CA014089). Dr Johnson acknowledges funding from NIH grant R01CA108614-06A1. AD, ZP and VM are partially supported by CIRM pre- and post-doctoral and F32 Developmental Biology training fellowship. NZ acknowledges the support of USC provost postdoctoral fellowship. ZB is Edgington Chair in Medicine and was supported by the Hastings Foundation.

### REFERENCES

- 1 Albanes D. Caloric intake, body weight, and cancer: a review. *Nutr Cancer* 1987; **9**: 199–217.
- 2 Calle EE, Rodriguez C, Walker-Thurmond K, Thun MJ. Overweight, obesity, and mortality from cancer in a prospectively studied cohort of US adults. *N Engl J Med* 2003; **348**: 1625–1638.
- 3 Qian Y, Fan JG. Obesity, fatty liver and liver cancer. *Hepatobiliary Pancreat Dis Int* 2005; **4**: 173–177.
- 4 Reddy JK, Rao MS. Lipid metabolism and liver inflammation. II. Fatty liver disease and fatty acid oxidation. *Am J Physiol Gastrointest Liver Physiol* 2006; **290**: G852–858.
- 5 Adinolfi LE, Rinaldi L, Guerrero B, Restivo L, Marrone A, Giordano M et al. NAFLD and NASH in HCV infection: prevalence and significance in hepatic and extra-hepatic manifestations. *Int J Mol Sci* 2016; **17**: E803.
- 6 Galicia VA, He L, Dang H, Kanel G, Vendryes C, French BA et al. Expansion of hepatic tumor progenitor cells in Pten-null mice requires liver injury and is reversed by loss of AKT2. *Gastroenterology* 2010; **139**: 2170–2182.
- 7 He L, Hou X, Kanel G, Zeng N, Galicia V, Wang Y et al. The critical role of AKT2 in hepatic steatosis induced by PTEN loss. *Am J Pathol* 2010; **176**: 2302–2308.
- 8 Horie Y, Suzuki A, Kataoka E, Sasaki T, Hamada K, Sasaki J et al. Hepatocyte-specific Pten deficiency results in steatohepatitis and hepatocellular carcinomas. *J Clin Invest* 2004; **113**: 1774–1783.
- 9 Stiles B, Wang Y, Stahl A, Bassilian S, Lee WP, Kim YJ et al. Liver-specific deletion of negative regulator Pten results in fatty liver and insulin hypersensitivity [corrected]. *Proc Natl Acad Sci USA* 2004; **101**: 2082–2087.
- 10 Xu X, Kobayashi S, Qiao W, Li C, Xiao C, Radaeva S et al. Induction of intrahepatic cholangiocellular carcinoma by liver-specific disruption of Smad4 and Pten in mice. *J Clin Invest* 2006; **116**: 1843–1852.
- 11 Chen CL, Uthaya Kumar DB, Punj V, Xu J, Sher L, Tahara SM et al. NANOG metabolically reprograms tumor-initiating stem-like cells through tumorigenic changes in oxidative phosphorylation and fatty acid metabolism. *Cell Metab* 2016; **23**: 206–219.
- 12 Li Y, He L, Zeng N, Sahu D, Cadenas E, Shearn C et al. Phosphatase and tensin homolog deleted on chromosome 10 (PTEN) signaling regulates mitochondrial biogenesis and respiration via estrogen-related receptor alpha (ERRalpha). *J Biol Chem* 2013; **288**: 25007–25024.

- 13 Rountree CB, Ding W, He L, Stiles B. Expansion of CD133-expressing liver cancer stem cells in liver-specific phosphatase and tensin homolog deleted on chromosome 10-deleted mice. *Stem Cells* 2009; **27**: 290–299.
- 14 Cho H, Mu J, Kim JK, Thorvaldsen JL, Chu Q, Crenshaw EB 3rd et al. Insulin resistance and a diabetes mellitus-like syndrome in mice lacking the protein kinase Akt2 (PKB beta). *Science* 2001; **292**: 1728–1731.
- 15 Garofalo RS, Orena SJ, Rafidi K, Torchia AJ, Stock JL, Hildebrandt AL et al. Severe diabetes, age-dependent loss of adipose tissue, and mild growth deficiency in mice lacking Akt2/PKB beta. *J Clin Invest* 2003; **112**: 197–208.
- 16 Taniguchi CM, Kondo T, Sajan M, Luo J, Bronson R, Asano T et al. Divergent regulation of hepatic glucose and lipid metabolism by phosphoinositide 3-kinase via Akt and PKClambda/zeta. *Cell Metab* 2006; **3**: 343–353.
- 17 He XC, Yin T, Grindley JC, Tian Q, Sato T, Tao WA et al. PTEN-deficient intestinal stem cells initiate intestinal polyposis. *Nat Genet* 2007; **39**: 189–198.
- 18 Chen CL, Tsukamoto H, Liu JC, Kashiwabara C, Feldman D, Sher L et al. Reciprocal regulation by TLR4 and TGF-beta in tumor-initiating stem-like cells. *J Clin Invest* 2013; **123**: 2832–2849.
- 19 Lee JS, Thorgeirsson SS. Genome-scale profiling of gene expression in hepatocellular carcinoma: classification, survival prediction, and identification of therapeutic targets. *Gastroenterology* 2004; **127**: S51–55.
- 20 Yamashita T, Wang XW. Cancer stem cells in the development of liver cancer. *J Clin Invest* 2013; **123**: 1911–1918.
- 21 Staal FJ, Luis TC. Wnt signaling in hematopoiesis: crucial factors for self-renewal, proliferation, and cell fate decisions. *J Cell Biochem* 2010; **109**: 844–849.
- 22 Emami KH, Nguyen C, Ma H, Kim DH, Jeong KW, Eguchi M et al. A small molecule inhibitor of beta-catenin/CREB-binding protein transcription [corrected]. *Proc Natl Acad Sci USA* 2004; **101**: 12682–12687.
- 23 Monga SP. beta-catenin signaling and roles in liver homeostasis, injury, and tumorigenesis. *Gastroenterology* 2015; **148**: 1294–1310.
- 24 Font-Burgada J, Shalpour S, Ramaswamy S, Hsueh B, Rossell D, Umemura A et al. Hybrid periportal hepatocytes regenerate the injured liver without giving rise to cancer. *Cell* 2015; **162**: 766–779.
- 25 Furuyama K, Kawaguchi Y, Akiyama H, Horiguchi M, Kodama S, Kuhara T et al. Continuous cell supply from a Sox9-expressing progenitor zone in adult liver, exocrine pancreas and intestine. *Nat Genet* 2011; **43**: 34–41.
- 26 Lamb JR, Zhang C, Xie T, Wang K, Zhang B, Hao K et al. Predictive genes in adjacent normal tissue are preferentially altered by sCNV during tumorigenesis in liver cancer and may rate limiting. *PLoS One* 2011; **6**: e20090.
- 27 Sung WK, Zheng H, Li S, Chen R, Liu X, Li Y et al. Genome-wide survey of recurrent HBV integration in hepatocellular carcinoma. *Nat Genet* 2012; **44**: 765–769.
- 28 Johnson DL, Stiles BL. Maf1, a new PTEN target linking RNA and lipid metabolism. *Trends Endocrinol Metab* 2016; **27**: 742–750.
- 29 Palian BM, Rohira AD, Johnson SA, He L, Zheng N, Dubeau L et al. Maf1 is a novel target of PTEN and PI3K signaling that negatively regulates oncogenesis and lipid metabolism. *PLoS Genet* 2014; **10**: e1004789.
- 30 Kalaany NY, Sabatini DM. Tumours with PI3K activation are resistant to dietary restriction. *Nature* 2009; **458**: 725–731.
- 31 Hardie DG, Schaffer BE, Brunet A, AMPK. An energy-sensing pathway with multiple inputs and outputs. *Trends Cell Biol* 2016; **26**: 190–201.
- 32 Inagawa S, Itabashi M, Adachi S, Kawamoto T, Hori M, Shimazaki J et al. Expression and prognostic roles of beta-catenin in hepatocellular carcinoma: correlation with tumor progression and postoperative survival. *Clin Cancer Res* 2002; **8**: 450–456.
- 33 Miyabayashi T, Teo JL, Yamamoto M, McMillan M, Nguyen C, Kahn M. Wnt/beta-catenin/CBP signaling maintains long-term murine embryonic stem cell pluripotency. *Proc Natl Acad Sci USA* 2007; **104**: 5668–5673.
- 34 Casali A, Batlle E. Intestinal stem cells in mammals and Drosophila. *Cell Stem Cell* 2009; **4**: 124–127.
- 35 Widelitz RB. Wnt signaling in skin organogenesis. *Organogenesis* 2008; **4**: 123–133.
- 36 Eckert C, Klein N, Kornek M, Lukacs-Kornek V. The complex myeloid network of the liver with diverse functional capacity at steady state and in inflammation. *Front Immunol* 2015; **6**: 179.
- 37 Gentzler R, Hall R, Kunk PR, Gaughan E, Dillon P, Slingluff CL Jr et al. Beyond melanoma: inhibiting the PD-1/PD-L1 pathway in solid tumors. *Immunotherapy* 2016; **8**: 583–600.
- 38 Spranger S, Bao R, Gajewski TF. Melanoma-intrinsic beta-catenin signalling prevents anti-tumour immunity. *Nature* 2015; **523**: 231–235.
- 39 Spranger S, Gajewski TF. Tumor-intrinsic oncogene pathways mediating immune avoidance. *Oncoimmunology* 2016; **5**: e1086862.
- 40 Domagala-Kulawik J. The role of the immune system in non-small cell lung carcinoma and potential for therapeutic intervention. *Transl Lung Cancer Res* 2015; **4**: 177–190.
- 41 Peng W, Chen JQ, Liu C, Malu S, Creasy C, Tetzlaff MT et al. Loss of PTEN promotes resistance to T cell-mediated immunotherapy. *Cancer Discov* 2016; **6**: 202–216.
- 42 Woo SR, Corrales L, Gajewski TF. Innate immune recognition of cancer. *Annu Rev Immunol* 2015; **33**: 445–474.

- 43 Moon BC, Hernandez-Ono A, Stiles B, Wu H, Ginsberg HN. Apolipoprotein B secretion is regulated by hepatic triglyceride, and not insulin, in a model of increased hepatic insulin signaling. *Arterioscler Thromb Vasc Biol* 2012; **32**: 236–246.
- 44 Janabi M, Yamashita S, Hirano K, Sakai N, Hiraoka H, Matsumoto K *et al*. Oxidized LDL-induced NF-kappa B activation and subsequent expression of proinflammatory genes are defective in monocyte-derived macrophages from CD36-deficient patients. *Arterioscler Thromb Vasc Biol* 2000; **20**: 1953–1960.
- 45 Kaler P, Augenlicht L, Klampfer L. Macrophage-derived IL-1beta stimulates Wnt signaling and growth of colon cancer cells: a crosstalk interrupted by vitamin D3. *Oncogene* 2009; **28**: 3892–3902.
- 46 Carpentier R, Suner RE, van Hul N, Kopp JL, Beaudry JB, Cordi S *et al*. Embryonic ductal plate cells give rise to cholangiocytes, periportal hepatocytes, and adult liver progenitor cells. *Gastroenterology* 2011; **141**: 1432–1438 e1431–1434.
- 47 Ueda S, Kawamata M, Teratani T, Shimizu T, Tamai Y, Ogawa H *et al*. Establishment of rat embryonic stem cells and making of chimera rats. *PLoS One* 2008; **3**: e2800.



This work is licensed under a Creative Commons Attribution-NonCommercial-NoDerivs 4.0 International License. The images or other third party material in this article are included in the article's Creative Commons license, unless indicated otherwise in the credit line; if the material is not included under the Creative Commons license, users will need to obtain permission from the license holder to reproduce the material. To view a copy of this license, visit <http://creativecommons.org/licenses/by-nc-nd/4.0/>

© The Author(s) 2017

Supplementary Information accompanies this paper on the Oncogene website (<http://www.nature.com/onc>)